

Predictions and Observations of Multiple Slip Modes in Atomic-Scale Friction

Sergey N. Medyanik,^{1,*} Wing Kam Liu,¹ In-Ha Sung,^{2,†} and Robert W. Carpick²

¹*Department of Mechanical Engineering, Northwestern University, Evanston, Illinois 60208, USA*

²*Department of Engineering Physics, University of Wisconsin–Madison, Madison, Wisconsin 53706, USA*

(Received 23 March 2006; published 27 September 2006)

Using the quasistatic Tomlinson model as a simple representation of an atomic force microscope, conditions for transitions in atomic-scale friction behavior from smooth sliding to single slips and then multiple slip regimes are derived based on energy minimization. The calculations predict and give a general explanation for transitions between different stick-slip regimes in the limit of low damping. The predictions are consistent with experimental observations of these transitions.

DOI: [10.1103/PhysRevLett.97.136106](https://doi.org/10.1103/PhysRevLett.97.136106)

PACS numbers: 68.37.Ps, 46.55.+d, 62.20.Qp, 81.40.Pq

Experimental studies of atomic-scale friction became possible with the invention of the atomic force microscope (AFM). AFM allows scanning of atomically flat surfaces with a nanoscale tip. One of the most striking features in AFM experiments is the observation of atomic lattice stick-slip behavior, where the lateral force exhibits a sawtooth form due to the sticking and subsequent rapid slip of the tip at repeated intervals corresponding to the lattice spacing of the crystalline sample [1].

Recently, Socoliuc *et al.* [2] observed with AFM the existence of smooth sliding with no stick-slip when the load was sufficiently low, and this corresponded with extremely low energy dissipation. As the load increased, a transition occurred to stick-slip behavior. In this and almost every other study, the periodicity is equal to one lattice spacing of the sample, and so we identify this regime as “single slip.” However, Johnson and Woodhouse have predicted that under certain conditions, slip may occur over an integer number of lattice spacings [3]. This is called a “multiple slip.” In fact, multiple slip was observed in the original Letter reporting atomic lattice stick-slip by Mate *et al.* [4], but has barely been discussed since.

Understanding transitions between different regimes of atomic-scale friction provides insight into the origins of friction, and may lead to the ability to control it. For example, it would be desirable to reliably maintain the ultralow dissipation observed in [2] to reduce energy dissipation and wear in micro- and nanoelectromechanical systems. Conversely, predictable stick-slip could be desirable for nanopositioning applications.

Idealized models have been extensively used by researchers to study stick-slip friction behavior [2,5–7]. It has long been established that the one-dimensional Tomlinson model for sliding of an elastically compliant system in a periodic potential [8] predicts an analytical condition for transition between smooth sliding and single-slip regimes [7]. However, there have been few attempts to specifically address the multiple slip regime, or the conditions that govern the transitions between different regimes of multiple slip. The notable study by Woodhouse

and Johnson [3] identified the relationships between the lateral (i.e., torsional) cantilever stiffness, the lateral stiffness of the elastically deformed contact itself, and the corrugation of the lateral force interaction, as the key parameters controlling the transition to multiple slips. An adjustable damping factor is included which represents the dynamic energy dissipation in the tip or sample materials, or in the cantilever itself. The transition from single-to-double slips occurs when high-frequency fluctuations in the lateral force triggered by the slip instability overshoot the corrugated lateral tip-sample interaction force. The possibility of overshoot reduces with increased damping. Recently, two further studies addressed the issue of multiple slips in atomic-scale friction. The first [9] investigated transitions between single and double slip modes and its dependence on damping, sliding velocity, and finite temperature by means of dynamical simulations. The other [10] dealt with the issues of the complex dynamics in atomic-scale friction, but also considered a quasistatic limit and transitions between multiple slip modes by solving the equation of motion numerically. However, despite this recent progress, a general analytical solution and experimental verification of transitions between the different slip regimes, especially for multiple slips, is still lacking, even for the simple case of the one-dimensional Tomlinson model in the quasistatic limit. We present this solution here, and compare with the first systematic experimental observations of the transition to multiple slips.

In this work, we examine the quasistatic energy landscape to develop a picture that describes the necessary conditions for various stick-slip mode transitions to occur. This governs not only the possibility of smooth-to-single [2,7] or the single-to-double [3,9] slip transitions, but transitions between *all* the possible modes, including the multiple slips of arbitrary integer slip values. The analysis is performed for the one-dimensional Tomlinson model. Conditions for the existence of different regimes of slip are derived based on the number of metastable states of the system. A transition from smooth sliding to stick-slip friction is intrinsic to this general solution as a special

case. Since we are examining the system statically, the transitions we discuss represent *possible* transitions. The behavior in a dynamic system will depend on the damping, the cantilever resonance frequency, the sliding speed, and the characteristic elastic velocity of the materials. The point of our analysis is to show that even before such dynamic aspects are considered, the energy landscape itself forbids specific regimes of slip in a manner that depends upon the load, cantilever stiffness, and the corrugation of the interfacial potential.

The monatomic tip scanning over the one-dimensional atomic chain [Fig. 1(a)] experiences a force due to the displacement applied to the spring base, which is coupled to the tip through the elastic spring of stiffness k . The spring represents the torsional stiffness of the AFM cantilever, and could also include the lateral stiffness of the tip structure and of the contact itself. The system is characterized by the following potential energy:

$$V = V_{\text{lat}} + V_{\text{spr}} = -\frac{E_0}{2} \cos\left(\frac{2\pi}{a} x_{\text{tip}}\right) + \frac{1}{2} k(x_{\text{tip}} - x_{\text{spr}})^2, \quad (1)$$

where E_0 is the amplitude, a is the periodicity, x_{tip} is the position of the tip, and x_{spr} is the equilibrium position of the spring. In (1), the total potential energy consists of two parts: V_{lat} represents the tip-substrate interaction, and V_{spr} is the linear elastic interaction between the tip and the spring. The equation of force equilibrium for the tip is $\partial V / \partial x_{\text{tip}} = 0$, thus:

$$\frac{E_0 \pi}{a} \sin\left(\frac{2\pi}{a} x_{\text{tip}}\right) = -k(x_{\text{tip}} - x_{\text{spr}}). \quad (2)$$

In (2), the left-hand side represents the lateral force, F_{lat} , acting on the tip due to the tip-substrate interaction, and the right-hand side represents the force due to the spring, F_{spr} . Thus, (2) can be rewritten as $F_{\text{lat}} = F_{\text{spr}}$.

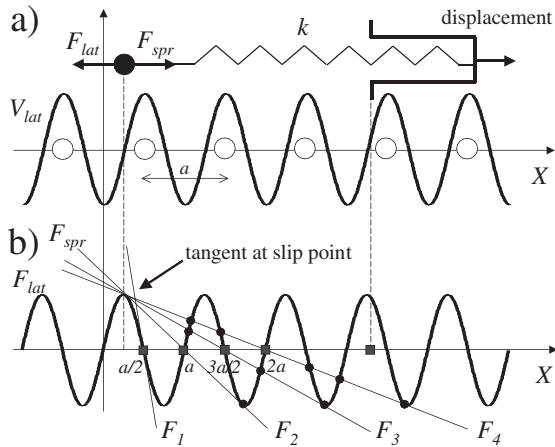


FIG. 1. (a) System configuration and periodic potential field. (b) Tip-substrate interaction force F_{lat} and spring forces F_i ($i = 1, \dots, 4$) corresponding to the critical stiffness values.

As shown in Fig. 1(b), slip occurs when F_{spr} is tangent to F_{lat} . This corresponds to the changeover from locally stable ($\partial^2 V / \partial x_{\text{tip}}^2 > 0$) to unstable ($\partial^2 V / \partial x_{\text{tip}}^2 \leq 0$) states. The whole process can be described as follows: as the spring base is moved in the $+x$ direction, the intersection point between F_{lat} and F_{spr} moves smoothly along the F_{lat} curve, which corresponds to the “sticking” stage. The system is in a local energy minimum. However, smooth movement cannot continue when F_{spr} becomes tangent to F_{lat} . The local equilibrium point changes to a point of unstable equilibrium. At this moment, the second derivative of the total energy is equal to zero (inflection point), and the tip slips to another available locally stable position. However, since a whole range of metastable states may be available, the “slipping” tip may skip one or several stable positions before it finally “sticks” to one particular equilibrium state. If the latter happens, we say that a *multiple slip* occurs. Where it comes to rest will be a function of the dynamics of the system, including the dissipation during sliding (with no dissipation, the tip would vibrate about the central spring position indefinitely). Depending on the number of possible metastable states, sliding may be classified into three categories: (1) smooth sliding (no stick-slip), (2) single-slip stick-slip, and (3) multiple slips. In the following, we investigate the number of possible metastable states of the system and derive conditions for transitions between different regimes.

The state of the system at the slip point is illustrated in Fig. 1(b), where several different positions of the spring base, corresponding to different values of the spring stiffness k , are considered. The number of intersection points between F_{lat} and F_{spr} depends on the inclination of the spring force, k , and changes at critical values $k = k_i$ that correspond to the spring forces $F_i = k_i(x_{\text{spr}} - x_{\text{tip}})$. Obviously, the number of solutions to the equilibrium equation changes only when the spring base is located in two types of positions: $x_{\text{spr}} = an$ and $x_{\text{spr}} = a(n + 1/2)$, $n = 0, 1, 2, \dots$. We consider the two cases by fixing the spring base at $x_{\text{spr}} = 0$ and assuming the tip position is a variable, $x_{\text{tip}} = x$, as follows. For the case $x_{\text{spr}} = an$, we assume $n = 0$ and adopting notations $A = E_0 \pi / a$, $\alpha = 2\pi / a$ rewrite (2) as $A \sin(\alpha x) = -kx$. For the case $x_{\text{spr}} = a(n + 1/2)$ we assume $n = 0$ and shift the interaction force by half a period, which first gives $A \sin[\alpha(x + \frac{a}{2})] = -kx$, and after simple algebraic manipulations, we find that $A \sin(\alpha x) = kx$. The two cases can be combined into one equation:

$$A \sin(\alpha x) = \pm kx, \quad (3)$$

where the spring stiffness k is assumed to be positive.

Depending on the values of A , α , and k , (3) can have different numbers of solutions, which always include the trivial solution, $x = 0$, corresponding to the global minimum of potential energy in the case of a very stiff spring.

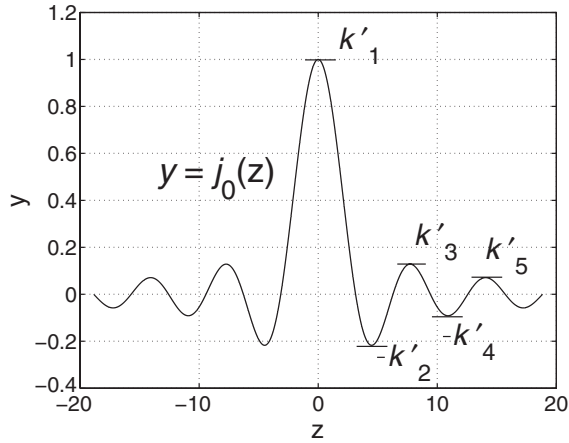


FIG. 2. Relationship between $j_0(z)$ and critical values k'_i .

Now we find nontrivial solutions of (3). Denoting $k' = k/(\alpha A)$ and $z = \alpha x$, we rewrite (3) as:

$$\frac{\sin(z)}{z} = \pm k'. \quad (4)$$

The function $\frac{\sin(z)}{z}$ is equal to the spherical Bessel function of the first kind, $j_0(z)$, which is shown in Fig. 2. It has zeros at $z = \pi l$, $l = \pm 1, \pm 2, \dots$ and is equal to 1 at $z = 0$. To investigate the number of solutions to (4), we have to examine the extrema of $j_0(z)$. No simple analytic relations exist for the zeros of the derivatives of the functions $j_n(z)$. However, representation in the form of McMahon's series expansion can be derived for the s th positive zero of $j'_0(z)$ ($z = 0$ counted as the first zero):

$$z_s = \beta - \beta^{-1} - \frac{2}{3}\beta^{-3} - \frac{32}{5}4438(8\beta)^{-5} - \dots, \quad (5)$$

where $\beta = \pi(s - \frac{1}{2})$. The first five values $k'_i = j_0(z_i)$, $i = 1, \dots, 5$ are 1.0, 0.2172, 0.1284, 0.0913, 0.0709.

Returning to our initial notation, we find:

$$k_i = \frac{2E_0\pi^2}{a^2} k'_i. \quad (6)$$

Figure 3 illustrates the energy landscapes corresponding to the first five critical stiffness values k_i , $i = 1, \dots, 5$. In each case (except for k_1), there are $i - 1$ local minima corresponding to the stable equilibrium states of the system

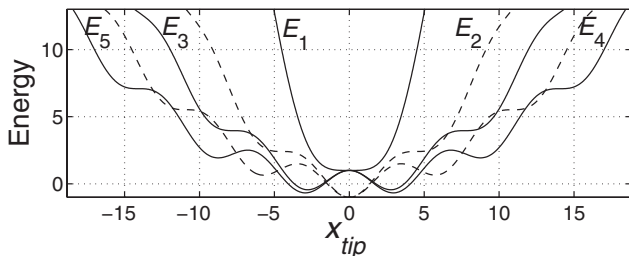


FIG. 3. Energy landscapes. E_i correspond to k_i , $i = 1, \dots, 5$.

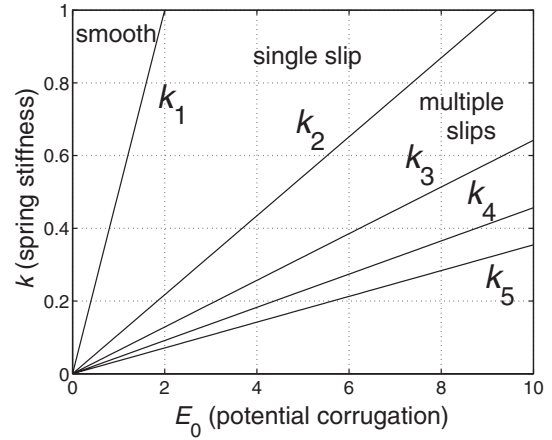


FIG. 4. Stick-slip opportunity map. Theoretical predictions.

and 2 inflection points corresponding to unstable equilibrium states. The system will slip from the unstable equilibrium on the left and will have i possible destinations to stick to. Thus, the spring stiffnesses k_i correspond to the critical values where the total number of possible slip destinations changes from $i - 1$ to i .

Among the critical stiffness values determined by (6), the first, $k_1 = 2E_0\pi^2/a^2$, is an important special case where a transition occurs from only one energy minimum at $k > k_1$ (a global minimum) to two local minima at $k < k_1$. Physically this means a possible transition from smooth sliding to a single-slip stick-slip regime. Introducing the parameter $\eta = 2E_0\pi^2/ka^2$, the tip movement is smooth when $\eta < 1$ and exhibits stick-slip when $\eta > 1$. This result was presented previously [2,7]. However, here we demonstrate that it is an integral part of a more general solution (6) which describes possible transitions between all multiples of slips. Introducing the parameter $\gamma_i = 1/k'_i$, transitions between stick-slip modes of different multiplicity can occur at $\eta = \gamma_i$. This is a necessary but not sufficient

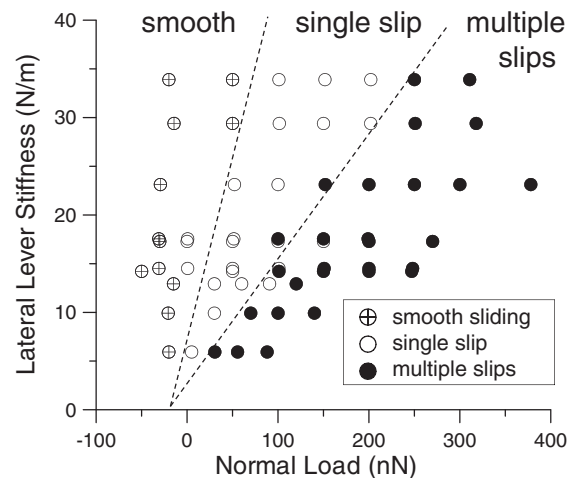


FIG. 5. Stick-slip friction map. Experimental results.

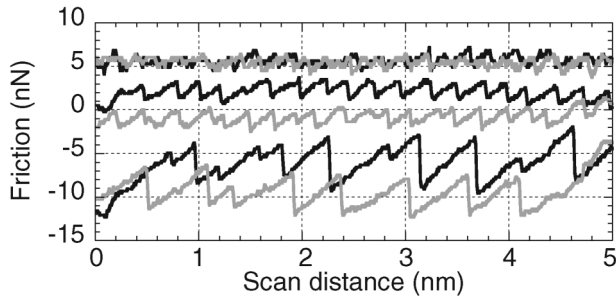


FIG. 6. Representative experimental friction behavior with increasing load (offset for clarity). Lateral force vs position traces demonstrate transitions from smooth sliding (top) to single (middle) and mostly double slips (bottom).

condition to observe multiple slips, since the dynamics and the damping will determine the observed slip multiplicity.

Figure 4 shows a “stick-slip opportunity map.” Here, spring stiffness k and potential corrugation E_0 are used as coordinate axes. Lines $k = k_i(E_0)$ given by (6) divide the whole space into areas where different types of atomic-scale friction have the possibility to exist: smooth sliding (no stick-slip), regular stick-slip (single slip), and multiple slips (double slips, triple slips, and so on). Figure 4 represents the maximum number of lattice sites that the tip can slip by. If the amount of damping is high, then even in a configuration where multiple slips are *possible*, the tip may only slip to the next local minimum, because damping prevents it from going further.

Figure 5 shows a similar map obtained from experimental observations using AFM, which are described in more detail in [11]. Here, the abscissa corresponds to the applied normal load instead of potential corrugation E_0 (Fig. 4). While the dependence of the potential corrugation on the load has not been measured, they are expected to be correlated and in fact were observed to be nearly linearly related in one case [2]. Our analysis indicates that indeed, for the data shown in Fig. 5, the potential corrugation increases with load.

The experiments were performed in air on the (0001) surface of a highly oriented pyrolytic graphite sample using Si AFM tips (Mikromasch USA) with a range of lateral and normal stiffnesses. These stiffnesses [12] and the friction calibration factor [13] were obtained experimentally. For each cantilever, friction was measured at different loads and classified according to the friction regime observed (Fig. 6). A close qualitative agreement between predictions and experimental results is apparent. It is not obvious that multiple slips should occur with increasing load. If continuum mechanics is valid at this scale, then increased load increases the lateral contact stiffness [14]. This increases the total stiffness of the system, k , moving the system

vertically on the map of Fig. 4, inhibiting multiple slips. The fact that transitions to more slips with increasing load are repeatedly observed demonstrates that any increase in total lateral stiffness is more than compensated for by the increased corrugation of the potential that occurs with increasing load.

The observation of multiple slips in the experiment indicates that we are not in a regime of high damping, which would restrict the stick-slip motion to the single-slip regime. A detailed examination of the damping present will be discussed separately [11].

The dynamic effects ignored in our theoretical analysis and the complex, uncertain atomic structure of the tip make quantitative comparison with experiments difficult. However, the strong qualitative agreement suggests that despite the model’s simplicity, conclusions drawn here may be applicable to other real systems.

The authors acknowledge support from NSF Grants No. CMS-0409688 and No. CMS-0409449. I.-H. Sung acknowledges support from the Korea Research Foundation, Grant No. M01-2004-000-20184-0.

*Currently at Washington State University, Pullman, WA, USA.

†Currently at Hannam University, South Korea.

- [1] S. Morita, S. Fujisawa, and Y. Sugawara, *Surf. Sci. Rep.* **23**, 1 (1996).
- [2] A. Socoliuc, R. Bennewitz, E. Gnecco, and E. Meyer, *Phys. Rev. Lett.* **92**, 134301 (2004).
- [3] K.L. Johnson and J. Woodhouse, *Tribol. Lett.* **5**, 155 (1998).
- [4] C.M. Mate, G.M. McClelland, R. Erlandsson, and S. Chiang, *Phys. Rev. Lett.* **59**, 1942 (1987).
- [5] D. Tomanek, W. Zhong, and H. Thomas, *Europhys. Lett.* **15**, 887 (1991).
- [6] J.N. Glosli and G.M. McClelland, *Phys. Rev. Lett.* **70**, 1960 (1993).
- [7] G.M. McClelland, in *Adhesion and Friction*, edited by M. Grunze and H.J. Kreuzer (Springer-Verlag, Berlin, 1989), Vol. 17, pp. 1–16.
- [8] G.A. Tomlinson, *Philos. Mag.* **7**, 905 (1929).
- [9] J. Nakamura, S. Wakunami, and A. Natori, *Phys. Rev. B* **72**, 235415 (2005).
- [10] W.G. Conley, A. Raman, and C.M. Krousgrill, *J. Appl. Phys.* **98**, 053519 (2005).
- [11] I.-H. Sung and R.W. Carpick (to be published).
- [12] C.P. Green, H. Lioe, J.P. Cleveland, R. Proksch, P. Mulvaney, and J.E. Sader, *Rev. Sci. Instrum.* **75**, 1988 (2004).
- [13] D.F. Ogletree, R.W. Carpick, and M. Salmeron, *Rev. Sci. Instrum.* **67**, 3298 (1996).
- [14] R.W. Carpick, D.F. Ogletree, and M. Salmeron, *Appl. Phys. Lett.* **70**, 1548 (1997).